Inorganic Chemistry

Article

pubs.acs.org/IC

Enhancement of Optical Faraday Effect of Nonanuclear Tb(III) Complexes

Takayuki Nakanishi,*[,†] Yuki Suzuki,[†] Yoshihiro Doi,[‡] Tomohiro Seki,[†] Hitoshi Koizumi,[†] Koji Fushimi,[†] Koji Fujita,[§] Yukio Hinatsu,[‡] Hajime Ito,[†] Katsuhisa Tanaka,[§] and Yasuchika Hasegawa*[,†]

[†]Faculty of Engineering and [‡]Faculty of Science, Hokkaido University, N13 W8, Kita-ku, Sapporo, Hokkaido 060−8628, Japan

[§]Graduate School of Engineering, Kyoto University, Katsura, Nishikyo-ku, Kyoto 615-8510, Japan

Supporting Information

ABSTRACT: The effective magneto−optical properties of novel nonanuclear Tb(III) complexes with Tb−O lattice (specifically, $[Tb_9(sal\text{-}R)_{16}(\mu\text{-}OH)_{10}]^+NO_3^-$, where sal-R = alkyl salicylate (R = $-CH_3$ (Me), $-C_2H_5$ (Et), $-C_3H_7$ (Pr), or $-C_4H_9$ (Bu)) are reported. The geometrical structures of these nonanuclear Tb(III) complexes were characterized using X-ray single-crystal analysis and shape-measure calculation. Optical Faraday rotation was observed in nonanuclear Tb(III) complexes in the visible region. The Verdet constant per Tb(III) ion of the Tb_9(sal-Me) complex is 150 times larger than that of general Tb(III) oxide glass. To understand their large Faraday rotation, electron paramagnetic resonance measurements of Gd(III) complexes were carried out. In this Report, the magneto−optical relation to the coordination geometry of Tb ions is discussed.

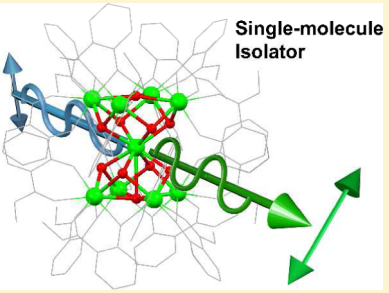

INTRODUCTION

Metal complexes with organic ligands have attracted much interest for optical,[1−4] electronic,[5,6] and magnetic[7−9] applications. In particular, polynuclear metal complexes show characteristic chemical and physical properties such as catalytic reactions,[10,11] magnetic coupling effects for single-molecular magnets,[12,13] and photosensitized luminescence between metal ions.[14,15] The molecular synthesis of polynuclear metal complexes is expected to open up a new field of advanced molecular science. Recently, polynuclear metal complexes composed of lanthanide ions with 4f orbitals have been synthesized, and their characteristic physical properties have been explored. Murugesu and Guo described the magnetic exchange coupling of binuclear Dy(III) complexes.[16,17] Piguet and co-workers reported the enhancement of the luminescence of polynuclear complexes by effective energy transfer from Cr(III) to lanthanide(III) ions.[18] We also recently demonstrated temperature-sensitive luminophores composed of Eu(III) and Tb(III) complexes.[19] Specific metal-to-metal interactions in polynuclear lanthanide complexes induce active magnetic and photophysical behavior.

Generally, lanthanide complexes show eight coordination structures, and their photophysical properties are dependent on the coordination geometry.[20] Additionally, the asymmetric coordination of lanthanides is also expected to have an effect on magnetic properties.[21] In this Paper, we hypothesize that the geometrical structures of polynuclear lanthanide complexes are related to their photomagnetic interaction with lanthanide ions. Recently, Ohkoshi reported the notable asymmetric structure of polynuclear Mn(II)−Nb(IV) compounds with metal ions and CN ligands.[22] They suggested that the asymmetric geometrical structure led to the enhancement of superexchange interactions in the magnetic field. Coordination geometry in polynuclear lanthanide complexes could be related to the photophysical and magneto−optical behaviors.

According to the magneto−optical behaviors of lanthanide compounds, we previously reported lanthanide inorganic materials, namely, EuX nanocrystals (X = O, S, and Se) composed of Eu(II) and chalcogenides ions.[23] The inorganic Eu−X lattices exhibit notable optical Faraday effect. The optical Faraday effect rotates the plane of polarized light in linear proportion to the component of the magnetic field in the direction of propagation. The Faraday effect is important for the construction of optical isolators for fiber-optic telecommunication systems.[24] The magneto−optical properties are induced in cubic Eu−X lattices. In contrast, lattice structures of polynuclear lanthanide complexes are dominated by organic ligand for construction of coordination structure. The Ln−O ordering bonds in polynuclear lanthanide complexes may provide novel aspects for the understanding of the optical Faraday effect.

The magnitude of the optical Faraday rotation angle is closely related to the magnetic exchange interaction of the materials.[23a] Hence, we focus on three-dimensional polynuclear Tb(III) complexes with ideal metal−oxygen lattice structures.[25] The effective Bohr magneton of Tb(III) ions is p = 9.72, which is larger than those of other paramagnetic metal ions (Eu(II): p = 7.94, Mn(II): p = 5.92, Fe(II): p = 4.90, Co(II): p = 3.87). The effective Bohr magneton of Tb(III) ions is expected to show specific magneto−optical properties in polynuclear Tb(III) complexes.

Received: April 23, 2014

   dx.doi.org/10.1021/ic5009363 | *Inorg. Chem.* XXXX, XXX, XXX−XXX

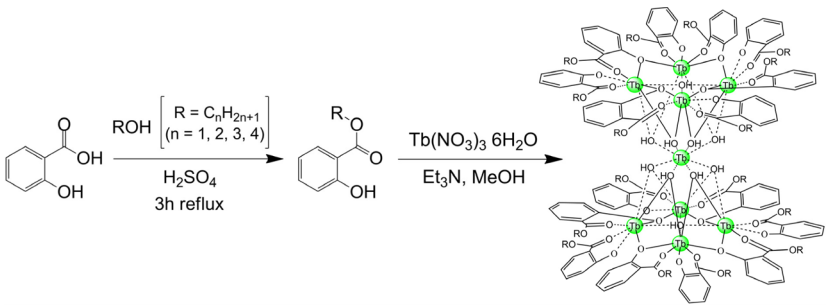

Figure 1. Preparation scheme of the nonanuclear Tb(III) complexes.

In this study, novel alkyl salicylate nonanuclear Tb(III) complexes with hourglass structure, namely, Tb_9(sal-R) and $[Tb_9(sal\text{-}R)_{16}(\mu\text{-}OH)_{10}]NO_3$, where sal-R = alkyl salicylate (R = $-CH_3$ (Me), $-C_2H_5$ (Et), $-C_3H_7$ (Pr), or $-C_4H_9$ (Bu)), are reported as shown in Figure 1. The Tb(III) complexes were prepared by the reaction of terbium nitrate with salicylates in methanol. The geometrical structures were analyzed using X-ray single-crystal analysis and shape-measure calculations.[26] We have successfully synthesized the Tb−O lattice using derivatives of salicylate ligands.[27] Optical Faraday rotation of nonanuclear Tb(III) complexes was observed in the visible region. This is the first observation of optical Faraday rotation in single lanthanide complexes. We also successfully estimated enhanced magnetic exchange interaction using electron paramagnetic resonance (EPR) measurement at room temperature. Novel nonanuclear Tb(III) complexes with magneto−optical properties are remarkable single molecules that directly connect with photophysical chemistry, coordination chemistry, and material science.

EXPERIMENTAL SECTION

Materials. Salicylic acid ($C_6H_4(OH)COOH$), methanol (CH_3OH), ethanol (C_2H_5OH), propanol (C_3H_7OH), and butanol (C_4H_9OH) were purchased from Kanto Chemical Co., Inc. Terbium(III) nitrate hexhydrate ($Tb(NO_3)_3{\cdot}6H_2O$), sulfuric acid (H_2SO_4), and triethylamine ($C_6H_{15}N$) were also purchased from Kanto Chemical Co., Inc. All other chemicals and solvents were reagent grade and were used without further purification.

Apparatus. ^{1}H NMR data were measured using an Auto-NMR JEOL ECS 400 MHz Spectrometer. ^{1}H NMR chemical shifts were determined using tetramethylsilane (TMS) as an internal standard. Electrospray ionization mass spectrometry (ESI-MS) measurements were made using Thermo Scientific Exactive. Fast atom bombardment mass spectrometry (FAB-MS) spectra were measured on JEOL JMS-700TZ. Elemental analyses were performed by MICRO CORDER JM10. Infrared spectra were recorded on a JASCO FT/IR-350 spectrometer. X-ray diffraction (XRD) spectra were characterized by a RIGAKU X-ray diffractometer RINT 2200. Single-crystal X-ray diffractions were made on a RIGAKU RAXIS RAPID imaging plate area detector. Quantitative elemental analysis was performed with inductively coupled plasma−atomic emission spectroscopy (ICP-AES). EPR spectra of nuclei Gd(III) complexes were measured using a JEOL JES-TE200 X-band ESR spectrometer.

Synthesis of Methyl Salicylate (Sal-Me). A solution of salicylic acid (3.0 g, 21.7 mmol) in 30 mL of methyl alcohol was added to sulfuric acid (1.0 mL), and after it was stirred and reacted for 5 h, distilled water (20 mL) was added to the reaction mixture. The pH value of this solution was adjusted to pH 7 by adding sodium carbonate. The mixture was extracted with ether (2 × 30 mL). The organic layer was separated and dried with magnesium sulfate, and the solvent was evaporated. The residue was chromatographed on silica gel eluting with ethyl acetate/hexane (35/65). Yield: 62.1%. ^{1}H NMR (400 MHz, $CDCl_3$, TMS): δ 3.95 (s, 3H: $-CH_3$), δ 6.86−6.99 (m, 2H: Ar), δ 7.43−7.48 (t, 1H: Ar), δ7.82−7.85 (d, 1H: Ar), δ10.7 (s, 1H: −OH) ppm. Selected IR (KBr, cm^{-1}): 1680(-C═O), 2960($-CH_3$). Elemental analysis calculated for $C_8H_8O_3$: C, 63.15%, H, 5.30%. Found: C, 63.12%, H, 5.35%. ESI-MS: m/z 151.04 $[M-H]^+$. Other salicylate derivatives, namely, Sal-Et, Sal-Pr, and Sal-Bu, were obtained using a similar synthesis to that of Sal-Me by changing alcohols EtOH, PrOH, and BuOH for MeOH, respectively.

Synthesis of Ethyl Salicylate (Sal-Et). Yield: 66.5%. ^{1}H NMR (400 MHz, $CDCl_3$, TMS): δ 1.39−1.42 (t, 3H: $-CH_3$), δ 4.40−4.46 (q, 2H: $-CH_2$), δ 6.92−6.97 (m, 2H: Ar),δ 7.51−7.55 (t, 1H: Ar),δ 7.85−7.88 (d, 1H: Ar), δ 10.8 (s, 1H: −OH) ppm. Selected IR (KBr, cm^{-1}): 1680(-C═O), 2930($-CH_2-$), 2960($-CH_3$). Elemental analysis calculated for $C_9H_{10}O_3$: C, 65.05%, H, 6.07%. Found: C, 65.14%, H, 6.18%. ESI-MS: m/z 165.06 $[M-H]^+$.

Synthesis of Propyl Salicylate (Sal-Pr). Yield: 60.1%. ^{1}H NMR (400 MHz, $CDCl_3$, TMS): δ 1.02−1.06 (t, 3H: $-CH_3$), δ 1.77−1.86 (m, 2H: $-CH_2$), δ 4.29−4.33 (t, 2H: $-CH_2$), δ 6.86−6.99 (m, 2H: Ar),δ 7.43−7.47 (t, 1H: Ar), δ 7.84−7.87 (d, 1H: Ar), δ 10.8 (s, 1H: −OH) ppm. Selected IR (KBr, cm^{-1}): 1680(-C═O), 2930($-CH_2-$), 2960($-CH_3$). Elemental analysis calculated for $C_{10}H_{12}O_3$: C, 66.65%, H, 6.71%. Found: C, 66.47%, H, 6.76%. ESI-MS: m/z 179.07 $[M-H]^+$.

Synthesis of Butyl Salicylate (Sal-Bt). Yield: 53.4%. ^{1}H NMR (400 MHz, $CDCl_3$, TMS): δ 0.97−1.01 (t,3H: $-CH_3$), δ 1.44−1.53 (m, 2H: $-CH_2$), δ 1.74−1.80 (m, 2H: $-CH_2$), δ 4.34−4.37 (t, 2H: $-CH_2$), δ 6.86−6.99 (m, 2H: Ar), δ 7.43−7.47 (t, 1H: Ar), δ 7.83−7.86 (d, 1H: Ar), δ 10.8 (s, 1H: −OH) ppm. Selected IR (KBr, cm^{-1}): 1680(-C═O), 2930($-CH_2-$), 2960($-CH_3$). Elemental analysis calculated for $C_{11}H_{14}O_3$: C, 68.02%, H, 7.27%. Found: C, 67.99%, H, 7.33%. ESI-MS: m/z 193.09 $[M-H]^+$.

Synthesis of Tb_9(sal-Me). Methyl salicylate (0.41 g, 2.7 mmol) was dissolved in methanol, and triethylamine (0.44 g, 4.40 mmol) was added to this solution with stirring at 40 °C. Then, $Tb(NO_3)_3{\cdot}6H_2O$ (0.686 g, 1.52 mmol) in methanol was added dropwise to this solution with further stirring for 20 min. White powder, Tb_9(sal-Me), $[Tb_9(sal\text{-}Me)_{16}(\mu\text{-}OH)_{10}]^+[NO_3]^-$, was obtained. Selected IR (KBr, cm^{-1}): 1382(NO_3), 1680 (-C═O), 2960 ($-CH_3$). Elemental analysis calculated for $C_{128}H_{122}O_{61}NTb_9$: C, 37.67%, H, 3.01%, N, 0.34%. Found: C, 37.97%, H, 3.14%, N, 0.31%. FAB-MS: m/z 4018.8 $[Tb_9(sal\text{-}Me)_{16}(\mu\text{-}OH)_{10}]^+$.

Synthesis of Tb_9(sal-Et). Ethyl salicylate (0.448 g, 2.7 mmol) was dissolved in methanol, and triethylamine (0.44 g, 4.40 mmol) was added to this solution with stirring at 40 °C. Then, $Tb(NO_3)_3{\cdot}6H_2O$ (0.686 g, 1.52 mmol) in methanol was added dropwise to this solution with further stirring for 20 min. White powder, Tb_9(sal-Et), $[Tb_9(sal\text{-}Et)_{16}(\mu\text{-}OH)_{10}]^+[NO_3]^-$), was obtained. Selected IR (KBr, cm^{-1}): 1382(NO_3), 1680(-C═O), 2930($-CH_2-$), 2960($-CH_3$). Elemental analysis calculated for $C_{148}H_{160}O_{61}NTb_9$: C, 40.17%, H, 3.61%, N, 0.33%. Found: C, 39.91%, H, 3.59%, N, 0.34%. FAB-MS: m/z 4242.2 $[Tb_9(sal\text{-}Et)_{16}(\mu\text{-}OH)_{10}]^+$.

Synthesis of Tb_9(sal-Pr). Propyl salicylate (0.486 g, 2.7 mmol) was dissolved in methanol, and triethylamine (0.44 g, 4.39 mmol) was added to this solution with stirring at 40 °C. Then, $Tb(NO_3)_3{\cdot}6H_2O$ (0.686 g, 1.52 mmol) in methanol was added dropwise to this solution with further stirring for 20 min. White powder, Tb_9(sal-Pr), [Tb_9(sal-

dx.doi.org/10.1021/ic5009363 | Inorg. Chem. XXXX, XXX, XXX−XXX

Pr)$_{16}$(μ-OH)$_{10}$]$^{+}$[NO$_3$]$^{-}$), was obtained. Selected IR (KBr, cm^{-1}): 1382(NO$_3$), 1680(-C═O), 2930(−CH$_2$−), 2960(−CH$_3$). Elemental analysis calculated for $C_{160}H_{186}O_{61}NTb_9$: C, 42.43%, H, 4.14%, N, 0.31%. Found: C, 42.12%, H, 4.10%, N, 0.34%. FAB-MS: m/z 4466.6 [Tb$_9$(sal-Pr)$_{16}$(μ-OH)$_{10}$]$^{+}$.

Synthesis of Tb$_9$(sal-Bu). Butyl salicylate (0.524 g, 2.7 mmol) was dissolved in methanol, and triethylamine (0.444 g, 4.39 mmol) was added to this solution with stirring at 40 °C. Then, Tb(NO$_3$)$_3$·6H$_2$O (0.686 g, 1.52 mmol) in methanol was added dropwise to this solution with further stirring for 20 min. White powder, Tb$_9$(sal-Bu), [Tb$_9$(sal-Bu)$_{16}$(μ-OH)$_{10}$]$^{+}$[NO$_3$]$^{-}$), was obtained. Selected IR (KBr, cm^{-1}): 1382(NO$_3$), 1680(-C═O), 2930(−CH$_2$−), 2960(−CH$_3$). Elemental analysis calculated for $C_{176}H_{218}O_{61}NTb_9$: C, 44.47%, H, 4.62%, N, 0.29%. Found: C, 44.16%, H, 4.57%, N, 0.51%. FAB-MS: m/z 4691.3 [Tb$_9$(sal-Bu)$_{16}$(μ-OH)$_{10}$]$^{+}$.

Synthesis of Gd$_9$(sal-Me). Gd(III) complexes were synthesized in a way similar to that of Tb$_9$(sal-Me) by using gadolinium(III) nitrate hexahydrate (Gd(NO$_3$)$_3$·6H$_2$O) in place of terbium(III) nitrate hexahydrate (Tb(NO$_3$)$_3$·6H$_2$O). Selected IR (KBr, cm^{-1}): 1382-(NO$_3$), 1680(-C═O), 2960(−CH$_3$). Elemental analysis calculated for $C_{128}H_{122}O_{61}NGd_9$: C, 37.81%, H, 3.02%, N, 0.34%. Found: C, 37.53%, H, 3.27%, N, 0.40%. FAB-MS: m/z 4002.0 [Gd$_9$(sal-Me)$_{16}$(μ-OH)$_{10}$]$^{+}$.

Synthesis of Gd$_9$(sal-Bu). Gd(III) complexes were synthesized in a way similar to that of Tb$_9$(sal-Bu) by using gadolinium(III) nitrate hexahydrate (Gd(NO$_3$)$_3$·6H$_2$O) in place of terbium(III) nitrate hexahydrate (Tb(NO$_3$)$_3$·6H$_2$O). Selected IR (KBr, cm^{-1}): 1382-(NO$_3$), 1680(-C═O), 2930(−CH$_2$−), 2960(−CH$_3$). Elemental analysis calculated for $C_{176}H_{218}O_{61}NGd_9$: C, 44.61%, H, 4.64%, N, 0.30%. Found: C, 44.40%, H, 4.73%, N, 0.33%. FAB-MS: m/z 4674.7 [Gd$_9$(sal-Bu)$_{16}$(μ-OH)$_{10}$]$^{+}$.

Synthesis of Tb(acac)$_3$. Terbium(III) acetate tetrahydrate (5.0 g, 12.3 mmol) was dissolved in distilled water (20 mL) by stirring. 2,4-Pentanedione (acac) (3.74 g, 37.4 mmol) was added dropwise to the above solution. The pH value of this solution was adjusted to pH 7 by adding NH$_3$ aqueous solution. The mixture produced a white precipitate after stirring for 3 h. The reaction mixture was filtered. The resulting white needle crystals of Tb(acac)$_3$, [Tb(acac)$_3$(H$_2$O)$_3$], were recrystallized from methanol. Yield: 69.9%. Selected IR (KBr, cm^{-1}): 920(C−CH$_3$), 1020(−CH$_3$), 1395(−CH$_3$), 1524(C═C), 1605(C═O). Elemental analysis calculated for $C_{15}H_{27}O_9Tb$: C, 35.31; H, 5.33%. Found: C, 35.31, H, 5.04%. ESI-MS: m/z 357.01 [Tb(acac)$_2$]$^{+}$.

Synthesis of Gd(acac)$_3$. Gd(acac)$_3$, Gd(acac)$_3$(H$_2$O)$_2$, was synthesized in a way similar to that of Tb(acac)$_3$ by using gadolinium(III) acetate tetrahydrate in place of terbium(III) acetate tetrahydrate. Yield: 38.1%. Selected IR (KBr, cm^{-1}): 920(C−CH$_3$), 1020(−CH$_3$), 1390(−CH$_3$), 1524(C═C), 1605(C═O). Elemental analysis calculated for $C_{15}H_{25}O_8Gd$: C, 36.72; H, 5.14%. Found: C, 36.52, H, 4.94%. ESI-MS: m/z 356.01 [Gd(acac)$_2$]$^{+}$.

Crystallography. Colorless single crystals of lanthanide complexes obtained from the solutions in methanol were mounted on a glass fiber by using epoxy resin glue. All measurements were made using a Rigaku RAXIS RAPID imaging plate area detector with graphite-monochromated Mo Ka radiation. Corrections for decay and Lorentz-polarization effects were made using empirical absorption correction, solved by direct methods, and expanded using Fourier techniques. Non-hydrogen atoms were refined anisotropically. Hydrogen atoms were refined using the riding model. The final cycle of full-matrix least-squares refinement was based on observed reflections and variable parameters. All calculations were performed using the crystal-structure crystallographic software package. We confirmed the CIF data by using the checkCIF/PLATON service. Additional crystallographic data are available in the Supporting Information.

Preparation of Polymer Films Containing Tb(III) Complexes and Faraday Rotation Measurements. The obtained Tb(III) clusters (70 mg) were added to a chloroform solution (5 mL). Then the solution (1 mL) was added to chloroform solution (8 mL) of poly(methyl methacrylate) (PMMA; 2.0 g). PMMA films were prepared on a glass substrate from the colloidal suspension via a casting method for the Faraday rotation measurements. The thickness of PMMA films was around 1.5 mm, and the transmittance was >90% in the 400−800 nm region. The Faraday effect measurements were performed using a measurement system for Faraday and Kerr effects (JASCO, Model K-250). A Xe lamp was used as the light source. The external magnetic field was 15 000 Oe.

RESULTS AND DISCUSSION

Structural Characterization of Nonanuclear Tb(III) Complexes. Nonanuclear Tb(III) complexes Tb$_9$(sal-R) (R = −CH$_3$ (Me), −C$_2$H$_5$ (Et), −C$_3$H$_7$ (Pr), and −C$_4$H$_9$ (Bu)) were synthesized by the complexation of the corresponding alkyl salicylate ligands, Sal-R (R = Me, Et, Pr, or Bu) with terbium nitrate in methanol under 40 °C. Their chemical structures were identified using NMR, IR, FAB-MS, and elemental analysis. All polynuclear Tb(III) complexes were composed of nine Tb(III) ions, 16 sal-R ligands, 10 OH parts, and one nitrate anion. The nonanuclear Tb(III) complexes (Tb$_9$(Sal-Me) and Tb$_9$(Sal-Bu)) were characterized using X-ray single-crystal analysis.

The resulting crystal data and their coordination structures are summarized in Figure 2 and Table 1. The nonanuclear

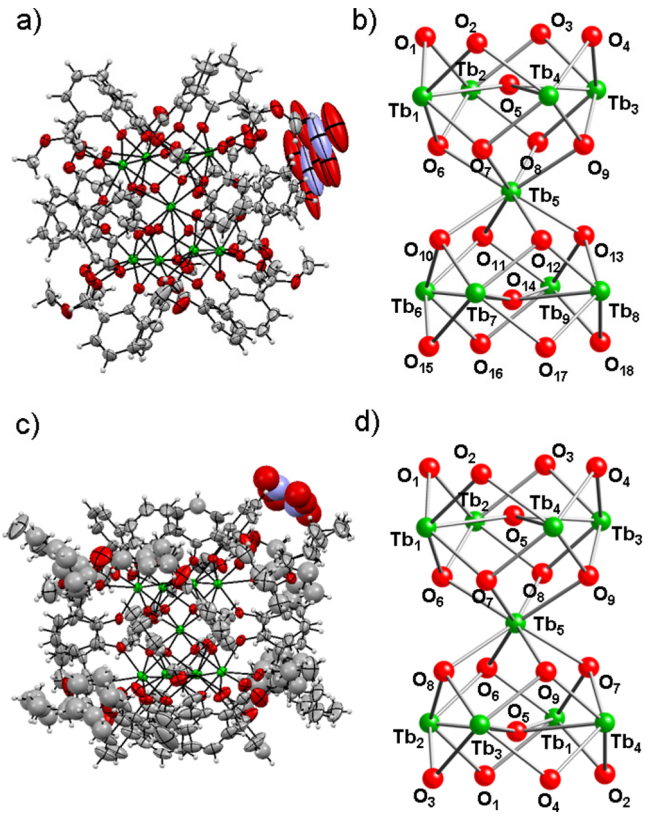

Figure 2. (a) ORTEP drawing of Tb$_9$(sal-Me). (b) Detailed view of the Tb−O framework in Tb$_9$(sal-Me). (c) ORTEP drawing of Tb$_9$(sal-Bu). (d) Detailed view of the Tb−O framework in Tb$_9$(sal-Bu).

Tb(III) complexes showed characteristic sandglass-shaped structures composed of nine Tb(III) ions, 16 salicylate ligands, eight bridged μ_3-OH^{-} parts, and two μ_4-OH^{-} parts. All Tb(III) ions are surrounded by eight oxygen, which is typical coordination number of lanthanide(III) complexes.

Selected angles and distances of Tb$_9$(Sal-Me) are shown in Figure 3a and Supporting Information, Tables S1 and S2. Selected angles α and γ in Tb$_9$(sal-Me) were found to be 90.39° and 97.11°, respectively. On the other hand, selected angle β

dx.doi.org/10.1021/ic5009363 | Inorg. Chem. XXXX, XXX, XXX−XXX

Table 1. Crystal Data of Tb(III) Complexes

	Tb_9(sal-Me)	Tb_9(sal-Bu)
chemical formula	$C_{128}H_{112}NO_{61}Tb_9$	$C_{176}H_{218}NO_{61}Tb_9$
formula weight	4070.59	4753.96
crystal color, habit	colorless, block	colorless, block
crystal system	monoclinic	orthorhombic
space group	$P2_1/n$ (#14)	$Pbcn$ (#60)
a/Å	21.5343(4)	29.0611(5)
b/Å	33.2157(7)	20.9836(4)
c/Å	21.7860(4)	31.5583(6)
α/deg	90.000	90.000
β/deg	90.0205(7)	90.000
γ/deg	90.000	90.000
V/Å3	15583.0(5)	19244.5(6)
Z	4	4
d_{calc}/g cm^{-3}	1.735	1.641
T/°C	−150.0	−150.0
m (Mo Kα)/cm^{-1}	41.021	33.345
max 2θ/deg	50.0	55.0
no. of measured reflections	119 678	184 917
no. of unique reflections	27 342	22 000
R ($I > 2s(I)$)[a]	0.0657	0.0693
R_w ($I > 2s(I)$)[b]	0.1574	0.1609

[a] $R = \Sigma||F_o| - |F_C||/\Sigma|F_o|$. [b] $R_w = [(\Sigma w(|F_o| - |F_c|)^2)/\Sigma wF_o^2]^{1/2}$

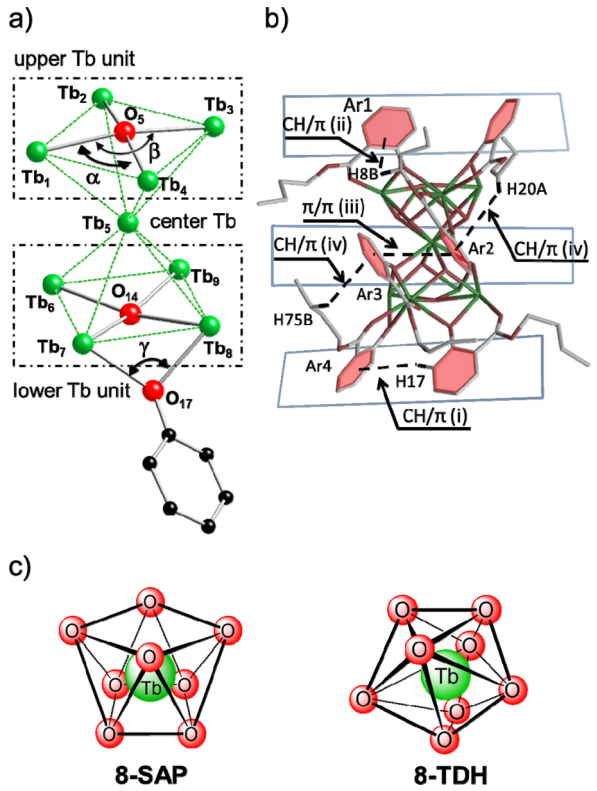

Figure 3. (a) Sandglass-shaped structure of Tb_9(sal-Me) and detailed view of the Tb−O−Tb angle. (b) Intramolecular CH−π interaction in Tb_9(sal-Bu). (c) Coordination structures of eight-coordinated square-antiprism (8-SAP) and eight-coordinated trigonal dodecahedron (8-TDH).

was estimated to be 169.20°. These Tb−O−Tb angles with nearly 90° or 180° lead to enhancement of magnetic interaction such as superexchange coupling of transition metal ions[28] and indirect exchange coupling of lanthanide ions.[29] Selected α, β, and γ angles for Tb_9(sal-Bu) are also listed in Supporting Information, Tables S3 and S4. The α, β, and γ angles are dependent on the chemical structures of the organic salicylate ligands. We also observed that the α, β, and γ angles of upper Tb(III) units ($Tb_{1,\ 2,\ 3\ and\ 4}$) are different than those of lower Tb(III) units ($Tb_{6,\ 7,\ 8\ and\ 9}$) in Tb_9(sal-Me) (Figure 3a). In contrast, the structures of the upper Tb units ($Tb_{1,\ 2,\ 3\ and\ 4}$) in Tb_9(sal-Bu) are the same as those of the lower Tb units. The structural differences between Tb_9(sal-Me) and Tb_9(sal-Bu) may result from the magnitude of the intramolecular CH−π, π−π interaction (Figure 3b and Supporting Information, Figure S5).

The selected distances and angles (Supporting Information, Tables S1−S4) are directly linked to the coordination geometry. On the basis of the crystal data, we carried out calculations on the shape factor S to estimate the degree of distortion for an ideal coordination structure.[26] The S value is given by

$$S = \min \sqrt{\left(\frac{1}{m}\right)\sum_{i=1}^{m}(\delta_i - \theta_i)^2} \quad (1)$$

where m, δ_i, and θ_i are the number of possible edges (m = 18 in this study), the observed dihedral angle between planes along the edge, and the dihedral angle for the ideal structure, respectively. The estimated S values of the complexes are summarized in Table 2. The coordination geometry of typical lanthanide complex has two characteristic geometries around the Tb(III) ions: the trigonal dodecahedron (8-TDH) with a D_{2d} point group and the square antiprism (8-SAP) with a D_{4d} point group, as shown in Figure 3c. The S values of the central Tb ions in Tb_9(sal-Me) were found to be 1.34° for 8-SAP and 14.45° for 8-TDH. From these results, the center Tb ion was

Table 2. Summary of Shape-Measure Calculations of the Tb_9(sal-Me) and Tb_9(sal-Bu)

Tb number of Tb_9(sal-Me)	S value for 8-TDH[a]: $S(D_{2d})$/deg.	S value for 8-SAP[b]: $S(D_{4d})$/deg.
Tb_1 (upper unit)	12.24°	16.84°
Tb_2 (upper unit)	13.13°	16.37°
Tb_3 (upper unit)	12.58°	16.16°
Tb_4 (upper unit)	12.37°	16.08°
Tb_6 (lower unit)	9.785°	17.85°
Tb_7 (lower unit)	11.36°	16.92°
Tb_8 (lower unit)	10.93°	17.21°
Tb_9 (lower unit)	10.73°	17.26°
$Tb_{1-4\ and\ 6-9}$	ave. 16.84°	ave. 11.64°
Tb_5 (center)	14.45°	1.34°
Tb number of Tb_9(sal-Bu)	S value for 8-TDH[a]: $S(D_{2d})$/deg.	S value for 8-SAP[b]: $S(D_{4d})$/deg.
Tb_1 (upper unit)	11.75°	18.58°
Tb_2 (upper unit)	11.33°	17.55°
Tb_3 (upper unit)	11.44°	19.38°
Tb_4 (upper unit)	11.07°	18.76°
Tb_6 (lower unit)	11.44°	19.38°
Tb_7 (lower unit)	11.07°	18.76°
Tb_8 (lower unit)	11.75°	18.58°
Tb_9 (lower unit)	11.33°	17.55°
$Tb_{1-4\ and\ 6-9}$	ave. 18.57°	ave. 11.40°
Tb_5 (center)	15.76°	1.92°

[a] 8-TDH: eight-coordinated trigonal dodecahedron. [b] 8-SAP: eight-coordinated square antiprism.

dx.doi.org/10.1021/ic5009363 | Inorg. Chem. XXXX, XXX, XXX−XXX

identified as 8-SAP with small S value. On the other hand, the S values of the eight Tb(III) ions of Tb_9(sal-Me) in the upper and lower units were found to be ave. 16.84° for 8-SAP and ave. 11.64° for 8-TDH. The eight Tb(III) ions in the upper and lower square units were classified as having 8-TDH structure. We also found that the S value of 8-TDH in the upper Tb unit of Tb_9(sal-Me) (ave. S value = 12.58°) was larger than those of the lower Tb units (ave. S value = 10.70°). The S values in the upper Tb unit in Tb_9(Sal-Bu) (ave. S value = 11.40°) were similar to those of the lower Tb units in Tb_9(sal-Bu) (ave. S value = 11.40°). The S value of the shape measure calculation is directly linked to the magnitude of the structural strain in coordination geometry. We propose that the structural strain of Tb_9(sal-Me) is larger than that of Tb_9(sal-Bu).

Faraday Effect on Nonanuclear Tb(III) Complexes. The wavelength dependence of the Faraday rotation angles was measured for PMMA thin films containing nonanuclear complexes Tb_9(sal-R) and mononuclear complex [Tb(acac)$_3$(H$_2$O)$_2$] (Figure 4). The Faraday spectrum at room

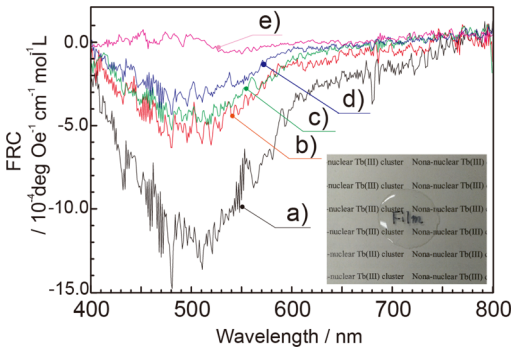

Figure 4. Faraday rotation spectra of PMMA film with Tb complexes (a) Tb_9(sal-Me), (b) Tb_9(sal-Et), (c) Tb_9(sal-Pr), (d) Tb_9(sal-Bu), and (e) Tb(acac)$_3$. (inset) Images of PMMA thin film containing Tb_9(sal-Me).

temperature with 15 000 Oe had clear negative peaks, which could have contributed to the 4f−4f transitions of Tb(III) ions in the Tb_9(sal-R) complexes. The Verdet constant V, which indicates the strength of the Faraday rotation, is calculated using

$$V = \theta/Hl \quad (3)$$

where θ, H, and l are the Faraday rotation angle (degrees), the external magnetic field, and the thickness of the thin film (cm), respectively. To estimate the Faraday rotation efficiency of nonanuclear Tb_9(sal-R) complexes, we normalize the Verdet constant in proportion to the Tb(III) concentrations, which are estimated by ICP-AES, and thus define Faraday rotation normalized by Tb(III) concentration (FRC) as

$$\mathrm{FRC} = \theta/(H \times l \times C) \quad (4)$$

where C is the Tb(III) concentration in the PMMA film containing Tb_9(sal-R) complexes. Tb_9(sal-Me) has the largest FRC value, which is $-16 \pm 2.0 \times 10^{-4}$/deg Oe^{1-} cm^{-1} mol^{-1} L, at around 511 nm (Table 3). On the other hand, the FRC values for Tb_9(Sal-Et), Tb_9(Sal-Pr), and Tb_9(Sal-Bu) are $-7 \pm 1.0 \times 10^{-4}$, $-6 \pm 1.0 \times 10^{-4}$, and $4 \pm 1.0 \times 10^{-4}$ /deg Oe^{1-} cm^{-1} mol^{-1} L, respectively. We also could not observe the effective Faraday effect of mononuclear [Tb(acac)$_3$(H$_2$O)$_2$]. From these results, we found that the Faraday rotation was enhanced with Tb−O clustering frameworks. The FRC value of standard optical borosilicate glass with Tb(III) ions is -0.10×10^{-4}/deg Oe^{1-} cm^{-1} mol^{-1} L at 633 nm. The Verdet value per Tb(III) ion of the Tb_9(sal-Me) complex is 150 times larger than that of general Tb(III) oxide glasses.[30] The orders of the FRC values for Tb_9(sal-R) complexes are consistent with that of inorganic single-crystal $Tb_3Al_5O_{12}$(TAG) and $Tb_3Ga_5O_{12}$ (TGG) with Tb−O lattices of cubic structure.[31] We have successfully observed the effective Faraday effects of single molecules. The Faraday rotation of $Tb_3Al_5O_{12}$ and $Tb_3Ga_5O_{12}$ are contributed to the edge of 4f−5d transitions. In contrast, the Faraday rotation of nonanuclear Tb(III) complexes might be due to the 4f−4f transition of Tb(III) ions, because of their characteristic Faraday rotation spectral shape at around 500 nm. We also observed that the optical Faraday rotation of Tb_9(Sal-Me) is larger than those of Tb_9(Sal-Et), Tb_9(Sal-Pr), and Tb_9(Sal-Bu). The magnitude of Faraday rotation might be related to the coordination geometry of Tb(III) ions. We consider that large strain of crystal structure of Tb_9(Sal-Me) affects the enhancement of Faraday rotation angles. The Faraday rotation angle is also based on the magnetic exchange interaction of materials.[23a]

Magnetic Exchange Interaction Estimated Using EPR Spectra. Magnetic exchange interaction at room temperature is a key factor for understanding the optical Faraday rotation of nonanuclear Tb(III) complexes. However, it is well-understood that the EPR signal of Tb(III) ions is not observed at $T > 30$ K because of the fast spin−lattice relaxation times that these ions have.[32] Here, we carried out EPR analysis using mononuclear [Gd(acac)$_3$(H$_2$O)$_2$] and nonanuclear Gd_9(sal-Me). The geometrical structure of nonanuclear Gd(III) clusters is the same as that of Tb_9(sal-Me) (see Supporting Information, Figure S1). The magnetic exchange interaction between lanthanide metals, H_e, is given by

$$\Delta H_{1/2} = H_d{}^2/H_e \quad (2)$$

where H_d and $\Delta H_{1/2}$ are the magnetic dipole interaction and the fwhm (full width at half-maximum) of the EPR spectrum, respectively. H_e can be estimated from $\Delta H_{1/2}$ using the EPR measurement. We observed the drastic difference of EPR signal

Table 3. Photomagnetic Properties of Tb(III) Complexes

sample	FRC[a] (10^{-4} deg Oe^{1-} cm^{-1} mol^{-1} L) (at λ_{max} nm)	FRC 10^{-4} deg Oe^{1-} cm^{-1} mol^{-1} L (at 633 nm)
Tb(acac)$_3$(H$_2$O)$_2$	−1.5 ± 0.5 (at 537 nm)	−0.4 ± 0.1
Tb_9(sal-Me)	−16 ± 2.0 (at 511 nm)	−2.5 ± 0.5
Tb_9(sal-Et)	−7 ± 1.0 (at 511 nm)	−1.2 ± 0.5
Tb_9(sal-Pr)	−6 ± 1.0 (at 511 nm)	−0.6 ± 0.5
Tb_9(sal-Bu)	−4 ± 1.0 (at 511 nm)	−0.4 ± 0.5
borosilicate glass[b](concentration of terbium: 26.5 mol %)		−0.10

[a]Tb(III) concentration-normalized Verdet constant. [b]Verdet constant of borosilicate glass is based on Tb(III) oxide.[30]

dx.doi.org/10.1021/ic5009363 | Inorg. Chem. XXXX, XXX, XXX−XXX

between mononuclear and nonanuclear Tb(III) complexes. The normal EPR spectra are shown in Figure 5. From this

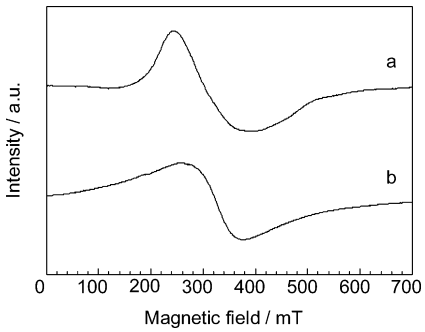

Figure 5. Normal and differential EPR spectra of Gd(III) complexes. (a) Mononuclear $[Gd(acac)_3(H_2O)_2]$. (b) Nonanuclear Gd_9(sal-Me).

observation, we consider that the equation can be applied to magnetic exchange interaction. The EPR spectra provide $\Delta H_{1/2}$ of Gd_9(sal-Me) was found to be 64.0 mT, which is smaller than 114.0 mT, the value for mononuclear $[Gd(acac)_3(H_2O)_2]$. Thus, we consider that magnetic exchange interaction H_e of Gd_9(Sal-Me) is much larger than that of mononuclear $[Gd(acac)_3(H_2O)_2]$. We consider that the nonanuclear Tb clusters with Tb−O lattices show through-space interaction (e.g., dipole−dipole interaction) for enhancement of the optical Faraday effect at room temperature.

SUMMARY AND CONCLUSIONS

We successfully observed the effective optical Faraday rotations of single Tb_9(sal-R) molecules. The nonanuclear Tb(III) clusters are much larger than those of previous Tb(III) oxide glass. On the other hand, Dy(III) or Ho(III) ions also have larger magnetic moments than Tb(III) ions (Dy(III): p = 10.63, Ho(III): p = 10.60). We are now studying the magnetization of Dy(III) and Ho(III) nonanuclear clusters and nonmagnetic Y(III) or Lu(III) nonanuclear clusters. Polynuclear molecules composed of Ln−O lattices are expected to open the novel Faraday materials with magneto−optical properties, using molecular science.

ASSOCIATED CONTENT

Supporting Information

Tb(III)−O−Tb(III) angle (deg) and Tb(III)−O bond length of Tb_9(sal-Me) and Tb_9(sal-Bu) (Tables S1−S4). CH−π distance of Tb_9(sal-Me) and Tb_9(sal-Bu) (Table S5), XRD profiles of Tb_9(sal-Me) and Gd_9(sal-Me) (Figure S1). This material is available free of charge via the Internet at http://pubs.acs.org. CCDC-956639 (Tb_9(sal-Me)) and 956692 (Tb_9(sal-Bu)) contain the crystallographic data for this Paper. These data can be obtained free of charge from The Cambridge Crystallographic Data Center via www.ccdc.cam.ac.uk/data_request/cif.

AUTHOR INFORMATION

Corresponding Authors

*E-mail: nakanishi@eng.hokudai.ac.jp. Phone/Fax: +81 11 706 7144. (T.N.)

*E-mail: hasegaway@eng.hokudai.ac.jp. (Y.H.)

Notes

The authors declare no competing financial interest.

ACKNOWLEDGMENTS

This work was partly supported by Grants-in-Aid for Scientific Research on Innovative Areas of "New Polymeric Materials Based on Element-Blocks (No. 2401)" (24102012) of the Ministry of Education, Culture, Sports, Science and Technology (MEXT) of Japan.

REFERENCES

(1) Bünzli, J.-C. G. *Chem. Rev.* **2010**, *110*, 2729−2755.
(2) Volger, A.; Kunkely, H. *Luminescent metal complex. Diversity of excited states in Transition metal and Rare Earth Compounds;* Splinger-Verlag: New York, 2001.
(3) Petoud, S.; Muller, G.; Moore, E.-G.; Xu, J.; Sokolnicki, J.; Riehl, J.-P.; Le, U.-N.; Cohen, S.-M.; Raymond, K.-N. *J. Am. Chem. Soc.* **2007**, *129*, 77−83.
(4) Blasse, G.; Grabmaier, B. C. *Luminescent Materials;* Splinger-Verlag: New York, 1994.
(5) Yu, X. M.; Zhou, G. J.; Lam, C. S.; Wong, W. Y.; Zhu, X. L.; Sum, J. X.; Wong, M.; Kwok, H. S. Kwok *J. Organomet. Chem.* **2008**, *693*, 1518−1527.
(6) Oyamada, T.; Kawamura, Y.; Koyama, T.; Sasabe, H.; Adachi, C. *Adv. Mater.* **2004**, *16*, 1082−1086.
(7) Scepaniak, J. J.; Harris, T. D.; Vogel, C. S.; Sutter, J.; Meyer, K.; Smith, J. M. *J. Am. Chem. Soc.* **2011**, *133*, 3824−3827.
(8) Zadrozny, J. M.; Xiao, D. J.; Atanasov, M.; Long, G. J.; Grandjean, F.; Neese, F.; Long, J. R. *Nature* **2013**, *5*, 577−581.
(9) Yamashita, K.; Miyazaki, R.; Kataoka, Y.; Nakanishi, T.; Hasegawa, Y.; Nakano, M.; Yamamura, T.; Kajiwara, T. *Dalton Trans.* **2013**, *42*, 1987−1990.
(10) Shimazaki, Y.; Nagano, T.; Takesue, H.; Ye, B. H.; Tani, F.; Naruta, Y. *Angew. Chem., Int. Ed.* **2004**, *43*, 98−100.
(11) Hou, Z.; Luo, Y.; Li, J.-X. *Organomet. Chem.* **2006**, *691*, 3114−3121.
(12) Ohkoshi, S.; Imoto, K.; Tsunobuchi, Y.; Takano, S.; Tokoro, H. *Nature* **2011**, *3*, 564−569.
(13) Lin, P. H.; Burchell, T. J.; Clérac, R.; Murugesu, M. *Angew. Chem., Int. Ed.* **2008**, *47*, 8848−8851.
(14) Li, Y.; Ren, S.; Liu, Q.; Ma, J.; Chen, X.; Zhu, H.; Dong, Y. *Inorg. Chem.* **2012**, *51*, 9629−9635.
(15) Torelli, S.; Imbert, D.; Cantuel, M.; Bernardinelli, G.; Delahaye, S.; Hauser, A.; Bünzli, J.-C. G.; Piguet, C. *Chem.—Eur. J.* **2004**, *10*, 3228−3242.
(16) Long, J.; Habib, F.; Lin, P.; Korobkov, I.; Enright, G.; Ungur, L.; Wernsdorfer, W.; Chibotaru, L. F.; Murugesu, M. *J. Am. Chem. Soc.* **2011**, *133*, 5319−5328.
(17) Guo, Y.; Xu, G.; Wernsdorfer, W.; Ungur, L.; Guo, Y.; Tang, J.; Zhang, H.; Chibotaru, L. F.; Powell, A. K. *J. Am. Chem. Soc.* **2011**, *133*, 11948−11951.
(18) Aboshyan-Sorgo, L.; Nozary, H.; Aebischer, A.; Bünzli, J.-C. G.; Morgantini, P.; Kittilstved, K. R.; Hauser, A.; Eliseeva, S. V.; Petoud, S.; Piguet, C. *J. Am. Chem. Soc.* **2012**, *134*, 12675−12684.
(19) Miyata, K.; Konno, Y.; Nakanishi, T.; Kobayashi, A.; Kato, M.; Fushimi, K.; Hasegawa, Y. *Angew. Chem., Int. Ed.* **2013**, *52*, 8848−8851.
(20) (a) Hasegawa, Y.; Tsuruoka, S.; Yoshida, T.; Kawai, H.; Kawai, T. *J. Phys. Chem. A* **2008**, *112*, 803−807. (b) Miyata, K.; Nakagawa, T.; Kawakami, R.; Kita, Y.; Sugimoto, K.; Nakashima, T.; Harada, T.; Kawai, K.; Hasegawa, Y. *Chem.—Eur. J.* **2011**, *17*, 521−528. (c) Kishimoto, K.; Nakagawa, T.; Kawai, T.; Hasegawa, Y. *Bull. Chem. Soc. Jpn.* **2011**, *82*, 148−154.
(21) (a) Lin, S. Y.; Wernsdorfer, W.; Unger, L.; Powell, A. K.; Guo, Y.; Tang, J.; Zhao, L.; Chibotaru, L. F.; Zhang, H. *Angew. Chem., Int. Ed.* **2012**, *51*, 12767−12771. (b) Bernot, K.; Luzon, J.; Bogani, L.; Etienne, M.; Sangregorio, C.; Shanmugam, M.; Caneschi, A.; Sessoli, R.; Gatteschi, D. *J. Am. Chem. Soc.* **2009**, *131*, 5573−5579. (c) Ishikawa, N.; Iino, T.; Kaizu, Y. *J. Am. Chem. Soc.* **2002**, *124*, 11440−11447.

(22) Nakagawa, K.; Imoto, K.; Miyahara, H.; Ohkoshi, S. *Polyhedron* **2013**, *52*, 424−428.
(23) (a) Hasegawa, Y.; Maeda, M.; Nakanishi, T.; Doi, Y.; Hinatsu, Y.; Fujita, K.; Hinatsu, Y.; Tanaka, K.; Koizumi, H.; Fushimi, K. *J. Am. Chem. Soc.* **2013**, *135*, 2659−2666. (b) Nakanishi, T.; Maeda, M.; Kawashima, A.; Fujita, K.; Tanaka, K.; Fushimi, K.; Hasegawa, Y. *J. Alloys Compd.* **2013**, *562*, 123−127. (c) Kawashima, A.; Nakanishi, T.; Shibayama, T.; Watanabe, S.; Fujita, K.; Tanaka, K.; Koizumi, H.; Fushimi, K.; Hasegawa, Y. *Chem.—Eur. J.* **2013**, *19*, 14438−14445. (d) Hasegawa, Y.; Thongchant, S.; Wada, Y.; Tanaka, H.; Kawai, T.; Sakata, T.; Mori, H.; Yanagida, S. *Angew. Chem., Int. Ed.* **2002**, *41*, 2073−2075. (e) Thongchant, S.; Hasegawa, Y.; Wada, Y.; Yanagida, S. *J. Phys. Chem. B* **2003**, *107*, 2193−2196. (f) Hasegawa, Y.; Afzaal, M. A.; O'Brien, P.; Wada, Y.; Yanagida, S. *Chem. Commun.* **2005**, 242−243. (g) Kataoka, T.; Tsukahara, Y.; Hasegawa, Y.; Wada, Y. *Chem. Commun.* **2005**, 6038−6040. (h) Hasegawa, Y.; Okada, Y.; Kataoka, T.; Sakata, T.; Mori, H.; Wada, Y. *J. Phys. Chem. B* **2006**, *110*, 9008−9011. (i) Hasegawa, Y.; Adachi, T.; Tanaka, A.; Afzaal, M.; O'Brien, P.; Doi, T.; Hinatsu, Y.; Fujita, K.; Tanaka, K.; Kawai, T. *J. Am. Chem. Soc.* **2008**, *130*, 5710−5715. (j) Tanaka, A.; Kamikubo, H.; Doi, Y.; Hinatsu, Y.; Kataoka, M.; Kawai, T.; Hasegawa, Y. *Chem. Mater.* **2010**, *22*, 1776−1781. (k) Tanaka, A.; Kamikubo, H.; Kataoka, M.; Hasegawa, Y.; Kawai, T. *Langmuir* **2011**, *27*, 104−108.
(24) (a) Furdyna, J. K. *J. Appl. Phys.* **1988**, *64*, R29−R64. (b) Gaj, J. A.; Ginter, J.; Galazka, R. R. *Phys. Status Solidi B* **1978**, *89*, 655−662. (c) Ohno, H.; Shen, A.; Matsukura, F.; Oiwa, A.; Endo, A.; Katsumoto, S.; Iye, Y. *Appl. Phys. Lett.* **1996**, *69*, 363−365. (d) Ohno, Y.; Young, D. K.; Beschten, B.; Matsukura, F.; Ohno, H.; Awschalom, D. D. *Nature* **1999**, *402*, 790−792. (e) Jungwirth, T.; Atkinson, W. A.; Lee, B. H.; MacDonald, A. H. *Phys. Rev. B* **1999**, *59*, 9818−9821. (f) Wang, Y.; Herron, N.; Moller, K.; Bein, T. *Solid State Commun.* **1991**, *77*, 33−38. (g) Norris, D. J.; Yao, N.; Charnock, F. T.; Kennedy, T. A. *Nano Lett.* **2001**, *1*, 3−7. (h) Jun, Y. W.; Jung, Y. Y.; Cheon, J. *J. Am. Chem. Soc.* **2002**, *124*, 615−619. (i) Schwartz, D. A.; Norberg, N. S.; Nguyen, Q. P.; Parker, J. M.; Gamelin, D. R. *J. Am. Chem. Soc.* **2003**, *125*, 13205−13218. (j) Stowell, C. A.; Wiacek, R. J.; Saunders, A. E.; Korgel, B. A. *Nano Lett.* **2003**, *3*, 1441. (k) Norberg, N. S.; Kittilstved, K. R.; Amonette, J. E.; Kukkadapu, R. K.; Schwartz, D. A.; Gamelin, D. R. *J. Am. Chem. Soc.* **2004**, *126*, 9387−9398. (l) Erwin, S. C.; Zu, L.; Haftel, M. I.; Efros, A. L.; Kennedy, T. A.; Norris, D. J. *Nature* **2005**, *436*, 91−94. (m) Beaulac, R.; Archer, P. I.; Liu, X.; Lee, S.; Salley, G. M.; Dobrowolska, M.; Furdyna, J. K.; Gamelin, D. R. *Nano Lett.* **2008**, *8*, 1197−1201.
(25) Mansekia, K.; Yanagida, S. *Chem. Commun.* **2007**, 1242−1244.
(26) (a) Binnemans, K.; Deun, R. V.; Görller-Walrand, C.; Collinson, S. R.; Martin, F.; Bruce, D. W.; Wickleder, C. *Phys. Chem. Chem. Phys.* **2000**, *2*, 3753−3757. (b) Hoard, J. L.; Silverton, J. V. *Inorg. Chem.* **1963**, *2*, 235−250. (c) Lippard, S. J.; Russ, B. J. *Inorg. Chem.* **1968**, *7*, 1686−1688. (d) Porai-Koshits, M. A.; Aslanov, L. A. *Russ. J. Struct. Chem.* **1974**, *13*, 244−253.
(27) (a) Manseki, K.; Hasegawa, Y.; Wada, Y.; Ichida, I.; Kanematsu, Y.; Kishida, T. *J. Lumin.* **2007**, *123*, 262. (b) Manseki, K.; Yanagida, S. *Chem. Commun.* **2007**, 1242−1244.
(28) (a) Kramers, H. A. *Physica* **1934**, *1*, 182−192. (b) Anderson, P. W. *Phys. Rev.* **1950**, *79*, 350−356.
(29) (a) Ruderman, M. A.; Kittel, C. *Phys. Rev.* **1954**, *96*, 99−102. (b) Kasuya, T. *Prog. Theor. Phys.* **1956**, *16*, 45−57. (c) Yoshida, K. *Phys. Rev.* **1957**, *106*, 893−898.
(30) Li, W.; Zou, K.; Lu, M.; Peng, B.; Zhao, W. *Int. J. Appl. Ceram. Technol.* **2010**, *7*, 369−374.
(31) (a) Kminskii, A. A.; Eichler, H. J.; Reiche, P.; Uecket, R. *Laser Phys. Lett.* **2005**, *2*, 489−492. (b) Geho, M.; Sekijima, T.; Fujii, T. *J. Cryst. Growth* **2004**, *267*, 188−193.
(32) Gafurov, M. R.; Ivanshin, V. A.; Kurkin, I. N.; Rodionova, M. P.; Keller, H.; Gutmann, M.; Staub, U. *J. Magn. Reson.* **2003**, *161*, 210−214.